Pergamon

Cement and Concrete Research 32 (2002) 1067–1070

CEMENT AND CONCRETE RESEARCH

Magnetic resonance imaging of ^{1}H, ^{23}Na, and ^{35}Cl penetration in Portland cement mortar

F. de J. Cano[a,b], T.W. Bremner[b], R.P. McGregor[a], B.J. Balcom[a,*]

[a]*MRI Centre, Department of Physics, University of New Brunswick, PO Box 4400, Fredericton, New Brunswick, Canada E3B 5A3*
[b]*Department of Civil Engineering, University of New Brunswick, PO Box 4400, Fredericton, New Brunswick, Canada E3B 5A3*

Received 12 April 2001; accepted 15 January 2002

Abstract

The first magnetic resonance imaging profiles of chloride content in low- and high-permeability Portland cement mortar have been obtained using a novel material science imaging technique. The penetration of water as well as chloride and sodium ions, into mortar specimens was monitored for a period of 72 h. Marked differences in penetration depth were observed in low- and high-permeability mortar. These preliminary experiments show significant differences between the extent and nature in the penetration of chlorides compared to water and sodium. © 2002 Elsevier Science Ltd. All rights reserved.

Keywords: Chloride penetration; Durability; Mortar; SPRITE-MRI; Transport properties

1. Introduction

Corrosion of the reinforcement is one of the main causes of deterioration of concrete structures [1]. Chloride penetration into concrete due to either diffusion or absorption is an important contributor to the corrosion of embedded steel in concrete. In northern countries, deicing salts are a major factor in the deterioration of highways and in all countries, chlorides from seawater exacerbate the deterioration process [2,3].

There are several tests used to measure the ability of concrete to resist chloride penetration. The rapid ASTM C 1202-94 test "Electrical Indication of Concrete's Ability to Resist Chloride Ion Penetration" determines the total electrical charge in Coulombs passed during a certain time. However, it does not simulate the transport of chloride ions in a real concrete structure. The AASHTO T259 "Resistance of Concrete to Chloride Penetration" 90-day ponding test, which involves diffusion and absorption of chlorides, is often used to determine the chloride diffusion coefficient. After the specified time, powder samples are obtained by drilling to specific depths and the chloride content is determined. This procedure gives a profile with low spatial resolution and is inherently destructive. In addition, slow chloride penetration in high-quality concrete and the crude resolution given by drilling may require the ponding test to continue for long durations.

It is desirable to have a nondestructive, high-resolution method to study the penetration of aggressive agents like chlorides into concrete. Magnetic resonance imaging (MRI) provides a unique way to nondestructively and with submillimetric resolution monitor the ingress of water and other species into concrete. Recently, a study of NaCl solution penetration into calcium silicate brick has been undertaken [4]. However, the traditional MRI techniques used have limitations on the shortest signal lifetime, T_2*, that can be observed and only proton and sodium profiles were obtained. In this communication, the SPRITE technique [5], which has shown an ability to image proton in a variety of materials with short T_2* times [6], is used to obtain the spatial distribution of ^{1}H, ^{23}Na, and for the first time, ^{35}Cl in Portland cement mortar as a function of location in a short time period.

2. SPRITE

Details about the SPRITE technique can be found elsewhere [5]. The signal intensity, S, from any point in the one-

---

* Corresponding author. Tel.: +1-506-453-4723x7938; fax: +1-506-453-4581.

E-mail address: bjb@unb.ca (B.J. Balcom).

0008-8846/02/$ – see front matter
PII: S0008-8846(02)00747-0

dimensional image, a profile, is related to the local nuclei density, ρ, by Eq. (1).

$$S = \rho e^{-\frac{t_p}{T_2*}} \left(\frac{1 - e^{-\frac{TR}{T_1}}}{1 - \cos\alpha e^{-\frac{TR}{T_1}}} \right) \sin\alpha \qquad (1)$$

where t_p is the phase encoding time, T_2* is effective spin–spin relaxation time, TR is the repetition time between radio frequency pulses, α is the flip angle, and T_1 is the spin lattice relaxation time. In Eq. (1) the term between brackets represents the steady-state longitudinal magnetization established after successive radio frequency pulses, and is valid for the hydrogen in water, which has spin $I = 1/2$. This term will have a more complex representation for sodium and chlorine nuclei, which have spin $I = 3/2$ [7].

This measurement technique, schematically outlined in Fig. 1, has been used to determine the water content and relaxation time mapping of drying concrete [8], and in the study of freezing and thawing of concrete [9].

3. Materials and methods

Quartz aggregates and white Portland cement were used to prepare mixes with *w/c* ratio of 0.6 and 0.3, which represent high- and low-permeability mortar. Cylindrical specimens measuring 30 mm in diameter were cast and moist cured for 3 days at 38 °C. After curing, the specimens were cut to 20 mm in length and oven dried at 110 °C for 1 day, which removed most of the evaporable water. Marine epoxy resin was then applied on the cylindrical exterior surface to make the penetration of NaCl solution unidirectional, as shown in Fig. 2.

Free induction decay and inversion recovery experiments were undertaken to estimate the bulk T_2* and T_1 relaxation times for ^{1}H, ^{23}Na, and ^{35}Cl in the specimens under study.

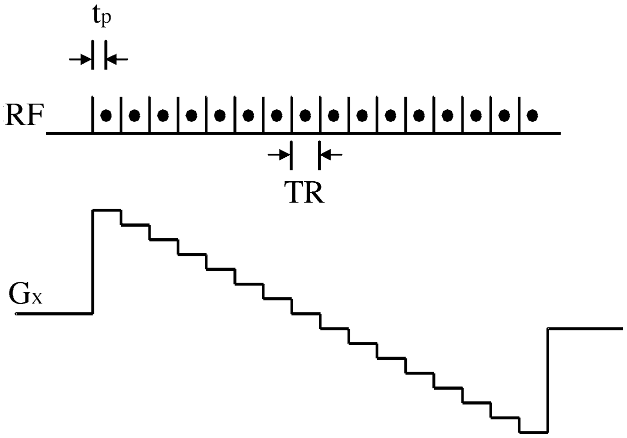

Fig. 1. One-dimensional SPRITE technique. The magnetic field gradient is ramped in 64 steps. A single data point is acquired at each gradient step at time t_p after the application of a radio frequency pulse, with flip angle α. The repetition time, TR, is the time between subsequent RF pulses at each gradient step.

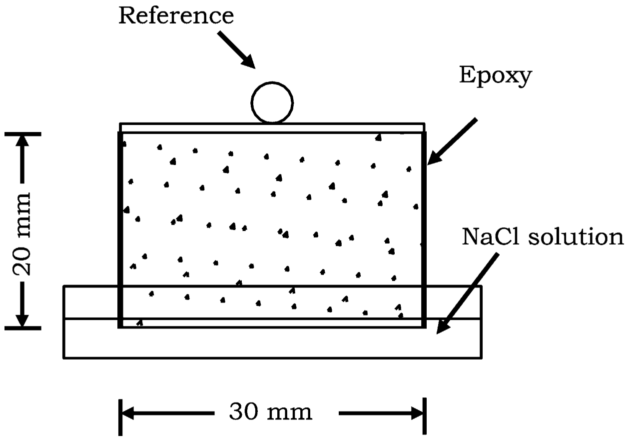

Fig. 2. Unidirectional NaCl solution uptake by 30-mm diameter and 20-mm length Portland cement mortar specimens. The concentration of the solution was 200 g/l of NaCl.

The SPRITE profiles were acquired using a Nalorac (Martinez, CA) 2.4-T, 32-cm bore, superconducting magnet with a water-cooled 8-cm i.d. microgradient insert. A birdcage type probe (Morris Instruments, Ottawa) was used for ^{1}H studies, whereas a newly designed probe was employed for ^{23}Na and ^{35}Cl. The spectrometer console was a Tecmag (Houston, TX) Apollo. The RF amplifier was a 2-kW AMT Model 3445 (Brea, CA).

After obtaining an initial "dry" profile of the ^{1}H distribution, the specimen was placed vertically into a shallow container and allowed to absorb NaCl solution from one end. The concentration of NaCl in the container was 200 g/l, which is approximately six times that of NaCl in seawater. SPRITE MRI measurements were performed at approximately 3, 20, and 72 h to monitor the penetration of the ^{1}H (water), ^{23}Na (Na^+), and ^{35}Cl (Cl^-). It should be noted that ^{37}Cl does not contribute to the signal, because its resonant frequency is different from the one corresponding to ^{35}Cl.

For each imaging experiment, a doped water or an NaCl solution reference was placed on the top of the specimen to permit scaling the profiles to compensate for small variations in the sensitivity of the instrument.

4. Results and discussion

The T_1 and T_2* relaxation times for ^{1}H, ^{23}Na, and ^{35}Cl in mortar at 72 h are given in Table 1. Both are well under 5 ms, which make SPRITE a convenient and, in some instances, required technique to image those species. The T_1 and T_2* relaxation times were single exponential, except for the T_2* for sodium and chlorine in mortar with *w/c* ratio of 0.6, where it has two components.

1D SPRITE profiles, with a field of view (FOV) of 100 mm and nominal resolution of 1.56 mm, were obtained and scaled to a reference sample. Figs. 3–5 show the distribution of ^{1}H, ^{23}Na, and ^{35}Cl at approximately 3, 20, and 72 h of NaCl solution absorption. The initial water content

Table 1
T_1 and T_2* relaxation times for ^{1}H, ^{23}Na, and ^{35}Cl in mortar

	T_1 (ms)[a]			T_2* (μs)[a]		
w/c	^{1}H	^{23}Na	^{35}Cl	^{1}H	^{23}Na	^{35}Cl
0.6	4.8	3.5	2.2	309	147[b] 755[c]	184[b] 917[c]
0.3	2.8	1.7	1.5	157	291	390

[a] Values at 72 h of NaCl solution absorption. All fitted relaxation times had uncertainties under 10% and, in some cases, much less.

[b] Short relaxation time component (contributes 31% and 29% to the total magnitude in ^{35}Cl and ^{23}Na, respectively).

[c] Long relaxation time component (contributes 69% and 71% to the total magnitude in ^{35}Cl and ^{23}Na, respectively).

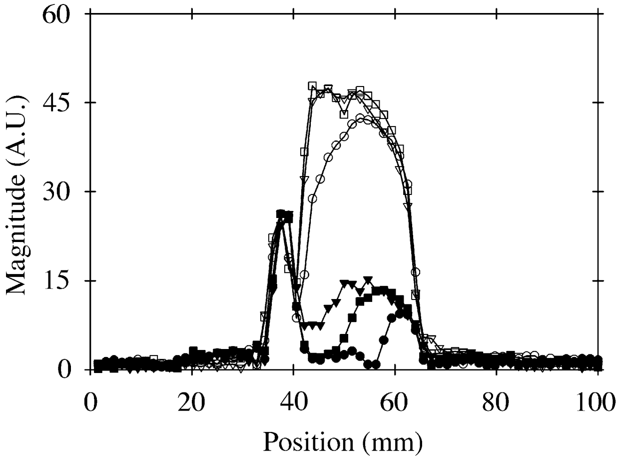

Fig. 4. ^{23}Na distribution in mortar specimens $w/c = 0.6$ at 4.3 h (○), 21.5 h (□), 72 h (▽), and $w/c = 0.3$ at 3.7 h (●), 20.3 h (■), and 72 h (▼). The parameters used for the SPRITE measurement were: FOV = 100 mm, $G_{\max} = 9.5$ G/cm, $t_p = 300$ μs, flip angle = 49°, scans = 2048, and acquisition time = 7.4 min.

of the specimens was found to be uniform and relatively low compared to the signal observed at 72 h.

As expected, the high permeability of mortar with $w/c = 0.6$ allows more rapid penetration of NaCl solution than the low-permeability ($w/c = 0.3$) specimen. Due to the advection created by the capillary absorption, both sodium and chloride ions tend to move with the absorbed water, thus, making diffusion negligible in the period studied.

As can be seen in these figures, all species have completely penetrated the high-permeability specimen in 3 h and there is only an increase in magnitude with time, which is related to the filling of smaller pores within the sample. Sodium exhibits almost the same behavior as water during the first few hours but at 72 h, the distribution of the three species in the specimen is quite different. One interesting feature of chlorides in high-permeability mortar, shown in Fig. 5, is the decrease in magnitude with time, which may be related to the chemical and physical binding of chlorides to the cement paste [10]. Chemically combined or bound chlorides possess a T_2* relaxation time much shorter than free chlorides and, therefore, they do not contribute to the signal observed.

In the low-*w/c* ratio specimen, the sodium exhibits also a behavior similar to water, but the penetration depth is always smaller. Pel et al. [4] also observed this behavior in their study. In spite of the high concentration of NaCl solution used, the low NMR sensitivity of ^{35}Cl made its observation difficult in this specimen. The signal to noise ratio is low compared to the one obtained in high-permeability mortar. The sensitivity for imaging chlorine in low-permeability mortar needs to be improved, which may be attained using a larger sample and/or a higher field magnet.

We also note the significant difference in imaging times required for sodium and chlorine compared to water, which

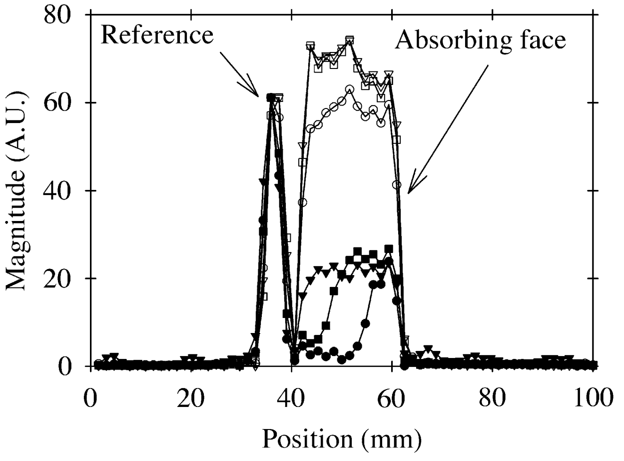

Fig. 3. ^{1}H distribution in mortar specimens $w/c = 0.6$ at 3.9 h (○), 20.8 h (□), 72 h (▽), and $w/c = 0.3$ at 3.3 h (●), 19.7 h (■), and 72 h (▼). The parameters used for the SPRITE measurement were: FOV = 100 mm, $G_{\max} = 7.5$ G/cm, $t_p = 100$ μs, flip angle = 9°, scans = 128, and acquisition time = 26 s.

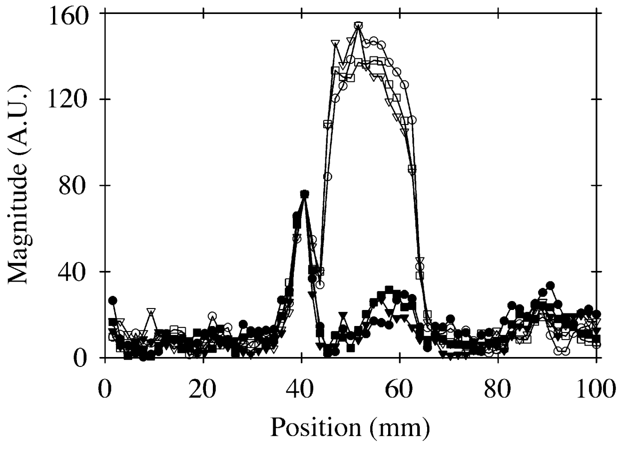

Fig. 5. ^{35}Cl distribution in mortar specimens $w/c = 0.6$ at 5 h (○), 22.2 h (□), 72 h (▽), and $w/c = 0.3$ at 4.5 h (●), 21.1 h (■), and 72 h (▼). The parameters used for the SPRITE measurement were: FOV = 100 mm, $G_{\max} = 25.6$ G/cm, $t_p = 300$ μs, flip angle = 44°, scans = 8192, and acquisition time = 20.7 min.

is mainly due to the lower NMR sensitivity of those nuclei, especially chlorine. To compensate for this, a larger number of signal averages were required to obtain a reasonable signal to noise ratio.

5. Conclusions

The SPRITE technique was successfully used to nondestructively and with millimetric resolution observe the penetration of water and sodium, and for the first time chlorides, into low- and high-permeability mortar.

The advection produced by the capillary absorption caused the sodium and chloride ions to move with the water. However, differences in the extent of penetration were observed in both types of mortar.

In the high-*w*/*c* ratio mortar specimen, it was possible to observe a decrease in magnitude with time, which may be related to the chemical and physical binding of chlorides to the cement paste.

The sensitivity of the measurement needs to be improved to image chlorides in low-*w*/*c* ratio mortar, an improvement which may be achieved either by the use of a larger specimen or a higher field magnet.

Work is in progress to improve the sensitivity of the measurement in low-*w*/*c* ratio mortar and eventually concrete specimens containing silica fume and fly ash will be used to image penetration of NaCl at a concentration similar to seawater.

Acknowledgments

B.J. Balcom acknowledges equipment and operating grants from NSERC, an NSERC Steacie Fellowship 2000–2002. F. de J. Cano acknowledges the leave of absence from the National Polytechnic Institute and the financial support from the Bank of Mexico and the National Council for Science and Technology of Mexico. The authors acknowledge useful discussions with Dr. Igor Mastikhin.

References

[1] P.K. Mehta, Durability—critical issues for the future, Concr. Int. 19 (7) (1997) 27–33.

[2] P.K. Mehta, T.W. Bremner, Concrete in the marine environment—some lessons for the future, in: P.K. Methta (Ed.), Proceedings of the O.E. Gjorv Symposium on Concrete for Marine Structures, ACI International, Farmington Hills, MI, 1996, pp. 175–190.

[3] Z.G. Matta, Concrete practices in the Arabian Gulf Region, Concr. Int. 20 (7) (1998) 51–52.

[4] L. Pel, K. Kopinga, E.F. Kaasschieter, Saline absorption in calcium-silicate brick observed by NMR scanning, J. Phys. D: Appl. Phys. 33 (2000) 1380–1385.

[5] B.J. Balcom, R.P. MacGregor, S.D. Beyea, D.P. Green, R.L. Armstrong, T.W. Bremner, Single point ramped imaging with T_1 enhancement (SPRITE), J. Magn. Reson., Ser. A 123 (1996) 131–134.

[6] B.J. Balcom, SPRITE imaging of short relaxation time nuclei, in: P. Blümer, B. Blümich, R. Botto, E. Fukushima (Eds.), Spatially Resolved Magnetic Resonance, Methods, Materials, Medicine, Biology, Rheology, Geology, Ecology, Hardware, Wiley-VCH, New York, 1998, pp. 75–86.

[7] V.F. Mitrovic, E.E. Sigmund, W.P. Halperin, Progressive saturation NMR relaxation, Phys. Rev. B 64 (2001) 1–7.

[8] S.D. Beyea, B.J. Balcom, P.J. Prado, A.R. Cross, C.B. Kennedy, R.L. Armstrong, T.W. Bremner, Relaxation time mapping of short T_2* nuclei with Single-Point Imaging (SPI) methods, J. Magn. Reson. 135 (1998) 156–164.

[9] P.J. Prado, B.J. Balcom, S.D. Beyea, T.W. Bremner, R.L. Armstrong, P.E. Grattan-Bellew, Concrete freeze/thaw as studied by magnetic resonance imaging, Cem. Concr. Res. 28 (2) (1998) 261–270.

[10] H.G. Midgley, J.M. Illston, The penetration of chlorides into hardened cement pastes, Cem. Concr. Res. 14 (4) (1984) 546–558.